Targeting Protein Translation in Human Non–Small Cell Lung Cancer via Combined MEK and Mammalian Target of Rapamycin Suppression

Marie-Emmanuelle Legrier,[1] Chia-Ping Huang Yang,[1] Han-Guang Yan,[1] Lluis Lopez-Barcons,[1,2] Steven M. Keller,[3] Roman Pérez-Soler,[2] Susan Band Horwitz,[1] and Hayley M. McDaid[1,2]

Departments of [1]Molecular Pharmacology and [2]Medicine, Albert Einstein College of Medicine, and [3]Department of Cardiothoracic Surgery, Montefiore Medical Center, Bronx, New York

Abstract

Lung cancer is a genetically heterogeneous disease characterized by the acquisition of somatic mutations in numerous protein kinases, including components of the rat sarcoma viral oncogene homolog (RAS) and AKT signaling cascades. These pathways intersect at various points, rendering this network highly redundant and suggesting that combined mitogen-activated protein/extracellular signal-regulated kinase (MEK) and mammalian target of rapamycin (mTOR) inhibition may be a promising drug combination that can overcome its intrinsic plasticity. The MEK inhibitors, CI-1040 or PD0325901, in combination with the mTOR inhibitor, rapamycin, or its analogue AP23573, exhibited dose-dependent synergism in human lung cancer cell lines that was associated with suppression of proliferation rather than enhancement of cell death. Concurrent suppression of MEK and mTOR inhibited ribosomal biogenesis by 40% within 24 h and was associated with a decreased polysome/monosome ratio that is indicative of reduced protein translation efficiency. Furthermore, the combination of PD0325901 and rapamycin was significantly superior to either drug alone or PD0325901 at the maximum tolerated dose in nude mice bearing human lung tumor xenografts or heterotransplants. Except for a PTEN mutant, all tumor models had sustained tumor regressions and minimal toxicity. These data (*a*) provide evidence that both pathways converge on factors that regulate translation initiation and (*b*) support therapeutic strategies in lung cancer that simultaneously suppress the RAS and AKT signaling network. [Cancer Res 2007;67(23):11300–8]

Introduction

Lung cancer is characterized by somatic mutations in many different protein kinases (1). Major components of the reticular activating system (RAS) and AKT signaling network are deregulated via genetic and epigenetic mechanisms in many human cancers including lung. In addition to p53, epidermal growth factor receptor and K-RAS are the most commonly acquired somatic mutations in both adenocarcinoma and bronchioalveolar carcinomas occurring in ~21% and 18% of patients, respectively.[4] PTEN is mutated in ~7% of non–small cell lung cancers (NSCLC), and by immunohistochemistry, ~25% of NSCLC tumors have lost PTEN protein expression, presumably by promoter methylation and/or loss of heterozygosity (2, 3). Somatic mutations in the phosphatidylinositol-4,5-bisphosphate 3-kinase (PI3K) catalytic subunit α occur in ~3% of NSCLC (1, 4).

Tumor growth is often dependent on the continued activation of one or two signaling pathways, termed oncogene addiction. Such tumors exhibit preferential sensitivity to pharmacologic inhibitors of these pathways (5). Thus, the development of effective therapies for many cancers, including lung, is dependent on accurate molecular classification.

There has been a longstanding interest in inhibitors that target aberrant mitogen-activated protein kinase (MAPK) signaling, precipitated by the finding that some cancer cell lines with B-RAF[V600E] mutations exhibit preferential sensitivity to mitogen-activated protein (MAP)/extracellular signal-regulated (ERK) kinase (MEK)-directed therapy (6). In melanoma, colorectal, and pancreatic cancers, somatic mutations of B-RAF are predominately localized to residue[V600E]; however, in lung cancer, this residue is mutated at a considerably lower frequency. Activating B-RAF mutations occur in ~3% of NSCLC (in squamous and adenocarcinoma histologies[4]) at two predominant locations, B-RAF[466−469] and B-RAF[597−600], the latter of which has been only identified in one human NSCLC cell line to date (7–9).

Inhibitors directed at components of RAS and AKT pathways are in various stages of development. CI-1040 (Pfizer) is an orally bioavailable and specific MEK inhibitor that has completed phase II clinical evaluation (10, 11). PD0325901 (Pfizer), a second generation MEK inhibitor, is currently undergoing clinical evaluation and has a significantly improved pharmacokinetic profile compared with CI-1040 (12). AKT signaling is highly pleiotropic (13), and although there are no PI3K-AKT inhibitors currently in the clinic, strides are being made in the development of effective candidates for therapeutic use (14, 15). One of the primary AKT effectors is the mTOR, a serine/threonine kinase that integrates mitogenic and nutrient signaling to regulate proliferation, cell cycle progression, mRNA translation, cytoskeletal organization, and survival (16). mTOR forms a rapamycin and nutrient-sensitive complex, mTORC1, and a second growth-factor sensitive and nutrient-sensitive complex, mTORC2 (reviewed in ref. 16). Rapamycin inhibits the function of mTORC1 by blocking the phosphorylation of two major downstream proteins: p70S6 kinase (p70S6K) and eukaryotic initiation factor (eIF) 4E-binding protein 1 (4E-BP1; refs. 17–19). Suppression of mTORC1 activates AKT kinase due to a negative feedback loop that exists

[4] http://www.sanger.ac.uk/genetics/CGP

between p70S6K and insulin receptor substate-1 (IRS1; ref. 16). AP23573 (Ariad) is a rapamycin analogue that is being evaluated in phase II clinical trials (20).

The genetic heterogeneity of lung cancer renders it a huge therapeutic challenge, compounded by the fact that the major signaling network that is deregulated, RAS-AKT, has complex positive and negative feedback control (21) and bifurcates at several levels (22–24). In signaling networks, it is unlikely that inhibition of only one component will confer therapeutic benefit, even in the presence of an "addicted" pathway. Thus, there is a strong rationale for multitargeted suppression of the RAS-PI3K/AKT network.

Herein, we test this logic using combined MEK and mTOR inhibitors in human NSCLC cell lines and tumor models grown in nude mice. Sensitivity to MEK-directed therapy was observed in non-V600E B-RAF mutant lung cancer cell lines, although at reduced sensitivity relative to B-RAF^{V600E} mutant cells. Synergism was observed in most cell lines except PTEN mutant H157 cells, and four of five tumor models evaluated had sustained tumor regressions after treatment with the combination relative to either MEK or mTOR inhibition alone. Mechanistically, combined suppression of MEK and mTOR potently dephosphorylated ribosomal protein S6$^{Ser235/236}$ and caused decreased ribosomal biogenesis and protein translation efficiency. These data substantiate accumulating evidence of a role for RAS, in addition to mTOR, in ribosomal protein S6 regulation through a highly conserved mechanism that oversees the rate of cellular proliferation.

Materials and Methods

Cell lines, antibodies, and reagents. Cells were purchased from the American Type Culture Collection, except H157 and H1703 that were obtained from National Cancer Institute (NCI)/Navy Medical Oncology [developed by H. Oie and Dr. F. Kaye (Bethesda, MD)]. Cells were cultured in RPMI containing 10% fetal bovine serum, penicillin (100 IU/mL), and streptomycin (100 μg/mL; Invitrogen). Experiments were performed using asynchronous cells grown in 10% serum to 70% to 80% confluence. All antibodies were from Cell Signaling Technologies except the following: AKT1/2, ERK1/2, and phospho-4E-BP1$^{ser65/Thr70}$ (Santa Cruz Biotechnology, Inc). Stock solutions of the MEK inhibitors CI-1040 and PD0325901 (Pfizer) were formulated in DMSO for *in vitro* experiments. The mTOR inhibitors AP23573 and rapamycin were obtained from Ariad Pharmaceuticals, Inc., and the Drug Synthesis and Chemistry Branch, NCI, respectively, and formulated in ethanol for *in vitro* experiments. LY294002 (Cell Signaling Technologies) was formulated in DMSO. Drugs were used at a final concentration of 0.03% to 0.06% vehicle. Unless stated otherwise, statistical analyses were performed using two-tailed unpaired Student's *t* tests.

Cell proliferation assay and multiple drug effect analysis. Cells were seeded at 2 to 3×10^4/mL, and serial dilutions of drugs were added after 2 h, for at least three cell doublings (72–120 h). Drug effects were measured using the CellTiter 96 AQueous nonradioactive cell proliferation assay (Promega) and Sulforhodamine B assays (25) and IC$_{50}$ determined. For AP23573, growth effects were described as IC$_{30}$ because rapamycin and its derivatives do not significantly impede cell proliferation. The nature of drug interaction was evaluated using the combination index (CI) method of Chou and Talalay (26) and the software Calcusyn (Biosoft).

Immunoblotting. Cells were treated with various concentrations of drugs corresponding to synergism. Lysates were extracted in denaturing lysis buffer, resolved on SDS-PAGE, and transferred to nitrocellulose.

Determination of caspase-mediated cell death. Drug-treated cells were incubated with CaspACE FITC-VAD-FMK (Promega), according to the manufacturer's instructions and counterstained with propidium iodide (Sigma Aldrich).

AKT kinase assay. Cells were treated with CI-1040, AP23573, or both, in the presence and absence of the PI3K inhibitor, LY294002. AKT kinase activity was determined from AKT immunocomplexes by analyzing phosphorylation of the substrate GSK-3 (Cell Signaling Technology), as described (27). Alternatively, AKT immunocomplexes were used in an *in vitro* kinase assay to catalyze the transfer of γ phosphate from [γ-32P] ATP (1 μmol/L Ci/μL) to 200 μmol/L of a specific Akt/SGK peptide (Upstate USA). Labeled peptides were precipitated, washed, and radioactive incorporation measured. Baseline values (lysates immunoprecipitated with immunoglobulin G alone) were subtracted before analysis.

Incorporation of ^{35}S-Methionine. Cells were treated with either CI-1040 or AP23593, or both for 24 to 72 h. One hour before harvesting, cells were grown in methionine-free medium (Invitrogen). [^{35}S]methionine (Amersham Biosciences) was added to a final concentration of 50 μCi/mL for 30 min. Cell pellets were precipitated, washed with trichloroacetic acid, and resuspended in 0.5 mol/L NaOH. Protein was transferred to glass microfiber filters (Whatman) for measurement of [^{35}S]-incorporation.

Linear sucrose gradient fractionation. Ribosomes were obtained after adding 0.1 mg/mL cycloheximide (Sigma) to drug-treated cells for 3 min and scraping cells into buffer, as described previously (28). Total ribosomes were obtained from equal quantities of S-30 proteins. Ribosomes were loaded onto 15% to 50% sucrose gradients and centrifuged at 39,000 rpm for 90 min at 4°C in a Beckman SW40Ti rotor. Gradient profiles were obtained by continuous UV monitoring at A$_{254}$. Alternatively, equal amounts of total ribosomes (A260) were loaded onto sucrose gradients and centrifuged as described above.

***In vivo* drug testing.** Human lung cancer xenograft and heterotransplanted tumor models were established in nude mice as described previously (29) and in compliance with institutional review board procedures. PD0325901 was formulated from powder as described previously for CI-1040 (29) and elsewhere (6). Rapamycin was made daily by diluting the stock solution in ethanol into a vehicle comprising 5% polyethylene glycol and 5% Tween 80 in saline. The final concentration of ethanol was 0.03%. Mice bearing tumors of ~ 300 to 600 mm^3 (n = 3–5 per treatment group) were treated daily with either 5 or 20 mg/kg PD0325901 p.o. and 0.5 to 1 mg/kg Rapamycin i.p. For combination treatments, drugs were given concurrently as 5 mg/kg PD0325901 p.o. with 1 mg/kg Rapamycin i.p. Control mice received vehicle alone for both drugs. Tumor volumes and weights were taken weekly and expressed relative to initial tumor volume. Mice were p.o. rehydrated with saline to relieve hyperkeratosis and diarrhea.

Results

Concurrent MEK and mTOR inhibition is synergistic in human NSCLC cell lines. Table 1 summarizes the genotype and sensitivity of cell lines to MEK and mTOR inhibitors. The B-RAF^{V600E} Colo205 cell line was used to compare drug sensitivity between V600E and non-V600E mutants that are common in NSCLC. There were three classes of response to MEK inhibition: hypersensitive (B-RAF^{V600E} mutant Colo205), sensitive (K-RAS mutant A549 and non-V600E B-RAF mutant NSCLC cell lines), and resistant (PTEN mutant H157 and p53 mutant H1703). This trend was more apparent with the highly specific inhibitor PD0325901, relative to CI-1040. Both H157 and H1703 cells have constitutively active AKT (CA-AKT), as described previously (30, 31); however, the underlying mechanism in H1703 has not been characterized. With the exception of H157, all cell lines had a comparable level of growth suppression after treatment with the mTOR inhibitor AP23573.

The combination of MEK and mTOR inhibitors was generally synergistic in all cell lines evaluated (Table 1 and Supplementary Fig. S1), except Colo205 that had an additive interaction. The nature of the interaction was dose dependent. Cells that were sensitive to MEK inhibition alone (B-RAF mutant NSCLC cell lines

Table 1. Concurrent MEK and mTOR inhibition is synergistic in human NSCLC cell lines

Cells	P53	B-RAF	K-RAS	IC$_{50}$ CI-1040 (μmol/L)	IC$_{50}$ PD0325901 (μmol/L)	IC$_{30}$ AP23573 (nmol/L)	Mean CI (± SD; FA, 0.2–0.8)
Colo205	Y103	V600E	Wild-type	0.31	~ 0.01	5.75	1.02 (±0.21)
H1755	C242	G469A	Wild-type	2.48	2	4.76	0.50 (±0.05)
H1395	Wild-type	G469A	Wild-type	6.43	8	4.11	0.51 (±0.13)
H1666	Wild-type	G466V	Wild-type	5.42	0.5	7.83	0.21 (±0.15)
A549	Wild-type	Wild-type	G12S	6.12	0.6	2.45	0.36 (±0.12)
H157 [*,†]	E298	Wild-type	G12R	13.5	>40	>20	0.97 (±0.55)
H1703 [†]	Intronic	Wild-type	Wild-type	12.6	>40	8.83	0.72 (±0.24)

NOTE: Mutation data were from the COSMIC[1] database. IC$_{50}$ and IC$_{30}$ are doses that result in 50% and 30% growth inhibition, respectively, relative to vehicle-only-treated control cells. Strict criteria were applied to drug interaction analyses, where synergism was defined as CI ≤ 0.7, additivity as 0.7 ≤ CI ≤ 1, and antagonism as CI ≥ 1. Data were expressed as mean CI (± SD), determined for a range of drug concentrations and a fractional effect (FA) of 0.2 to 0.8. Supporting data summarizing the nature of the drug interaction with dose range are presented in Supplementary Fig. S1 for some cell lines.
*PTEN G251C mutant.
† CA-AKT.

and A549) had a more pronounced synergistic interaction compared with cell lines that were resistant (H1703 and H157). B-RAF^{G466V} H1666 cells had a highly synergistic interaction, evident at very low drug concentrations over a wide range (Supplementary Fig. S1). H157 and H1703 had variable levels of synergy, although over a wider dose range, the nature of the interaction was generally additive, reflected in higher mean CI values (Table 1). Synergism was also observed in A549 for CI-1040 with rapamycin (Supplementary Fig. S1B) and also for the highly specific MEK inhibitor PD0325901 with either Rapamycin or AP23573 [mean CI (± SD) over a fractional effect range of 0.2–0.8: PD0325901 with rapamycin, 0.003 (±0.009); PD0325901 with AP23573, 0.004 (±0.008)].

A B-RAF^{V600E} mutant cell line Colo205 was hypersensitive to MEK-directed therapy, in agreement with Solit et al. (6). This is a high activity B-RAF mutant that strongly activates ERK signaling (8). However, combined MEK and mTOR inhibition was additive in this cell line, presumably due to its hypersensitivity to MEK inhibition alone. The B-RAF^{G469A} mutant cell lines H1755 and H1395, also classified as high activity B-RAF mutants, although not to the same extent as B-RAF^{V600E}, are sensitive to MEK inhibition and synergize with mTOR inhibitors (Table 1). The B-RAF^{G466V} mutation present in H1666 cells is an impaired activity mutant because it activates ERK through heterodimerization with C-RAF (8) and is defective in directly phosphorylating MEK. H1666 cells are the only human NSCLC cell line known to contain this mutation; thus, the widespread effect of the combination in this genotype could not be evaluated.

Expression of proteins downstream of MEK and mTOR. The MEK inhibitor CI-1040, either alone or in combination, was associated with dephosphorylated ERK$^{Thr202/Tyr204}$ (Fig. 1A). p70S6K is one of the best characterized downstream signaling components of mTORC1 (32) and exists as 85 and 70 kDa species corresponding to location in the nucleus and cytoplasm, respectively. AP23573 dephosphorylated p70S6K^{Thr389} in all cell lines except H1666 that may express a resistant variant of mTORC1. Decreased p70S6K^{Thr389} phosphorylation by MEK inhibitors has been noted elsewhere, although under conditions of phorbol 12-myristate 13-acetate stimulation using U0126 (23), however, this was not observed here with CI-1040. Doses of CI-1040 exceeding

10 μmol/L caused diminished expression of total ERK, AKT, and p70S6K (data not shown). These were nonspecific effects due to excessively high concentrations of the inhibitor.

Expression of proteins implicated in feedback regulation of MEK and mTOR. CI-1040 treatment caused increased phosphorylation of MEK$^{Ser217/221}$ in all cell lines analyzed, although in B-RAF mutant H1666 cells, basal levels were higher and more moderate changes in MEK$^{Ser217/221}$ phosphorylation were observed. This suggests that all cell lines undergo feedback activation of RAS in response to MEK inhibition. CI-1040–induced changes in phosphorylation of MEK at RAS-independent sites, (Thr^{286} and Ser^{298}) did not occur.

Full activity of AKT requires phosphorylation at Ser^{473} and Thr^{308} that is mediated by mTORC2 and phosphoinositide-dependent kinase 1, respectively (reviewed in ref. 16). CI-1040 and AP23573 both caused increased phosphorylation of pAKT^{ser473} and pAKT^{Thr308} in A549 and H1703 cells (Fig. 1B), consistent with our previous observations (29). H1666 cells had intrinsically low expression of Ser^{473} and Thr^{308} that was unchanged after CI-1040 or AP23573 treatment. PTEN mutant H157 cells had high CA-AKT, and small increases in pAKT^{ser473} and pAKT^{Thr308} phosphorylation were observed by both CI-1040 or AP23573 but not in combination treatments (Fig. 1B).

Drug-induced AKT kinase activation. AKT kinase activity also increased, as shown for A549 (Fig. 1C). CI-1040 induced low-level AKT activation (~1.4–2-fold) at concentrations associated with synergy. AP23573 induced AKT kinase activation in A549 cells (Fig. 1C and D) and in H1703 and H157 cells (data not shown), consistent with published data that attributes this effect to feedback regulation by insulin-like growth factor I via IRS1 (27). Consistent with this, AKT kinase activation by either AP23573 or CI-1040 was abolished in serum-free conditions (data not shown). In A549, the combination of both drugs also resulted in AKT kinase activation.

Both CI-1040– and AP23573-mediated AKT kinase activation was partially attributable to PI3K because the specific PI3K inhibitor, LY294002, partially inhibited this effect (Fig. 1D). Low concentrations of LY294002 were used to prevent the inhibition of other kinases including mTOR.

Concurrent inhibition of MEK and mTOR suppresses proliferation but does not enhance cell death. Doubling time was determined as a measure of cell proliferation rates (Table 2). Data for the B-RAF^{V600E} mutant cell line Colo205 is also included. CI-1040 or AP23573 alone had differential effects, depending on the genotype of each cell line; however, combined treatment significantly increased doubling time in all cell lines, consistent with suppression of proliferation. This suggests that the RAS and AKT/mTOR pathways converge to regulate cellular proliferation through a highly conserved mechanism because this phenotype was observed regardless of cellular genotype. Note that for A549 cells, the effects of the combination were less pronounced relative to the other cell lines, presumably due to their rapid proliferation rate.

The effect of either CI-1040 or AP23573 on cell cycle distribution, cyclin D1, and P27/$^{kip-1}$ varied, depending on the genotype (Supplementary Fig. S2). The combination of MEK and mTOR inhibition caused G_0-G_1 arrest in all cell lines, although suppression of proliferating cell nuclear antigen (PCNA) by the combination, relative to either drug alone, was significant only in A549 and H157 cells. Thus, p27/$^{kip-1}$, cyclin D1, or PCNA were not universally prognostic of response to CI-1040, AP23573, or the combination; however, decreased doubling time and G_0-G_1 arrest were observed in all cells treated with the combination.

Cells that were sensitive to MEK inhibition (A549 and H1666) had caspase-mediated cell death in response to CI-1040 alone (Fig. 2A); however, this was not potentiated by the addition of an mTOR inhibitor. Autophagy is a mode of cell death associated with mTOR suppression; however, there was no enhancement of autophagic cell death by the addition of CI-1040 (data not shown). Thus, potentiation of cell death was not a major effect of or
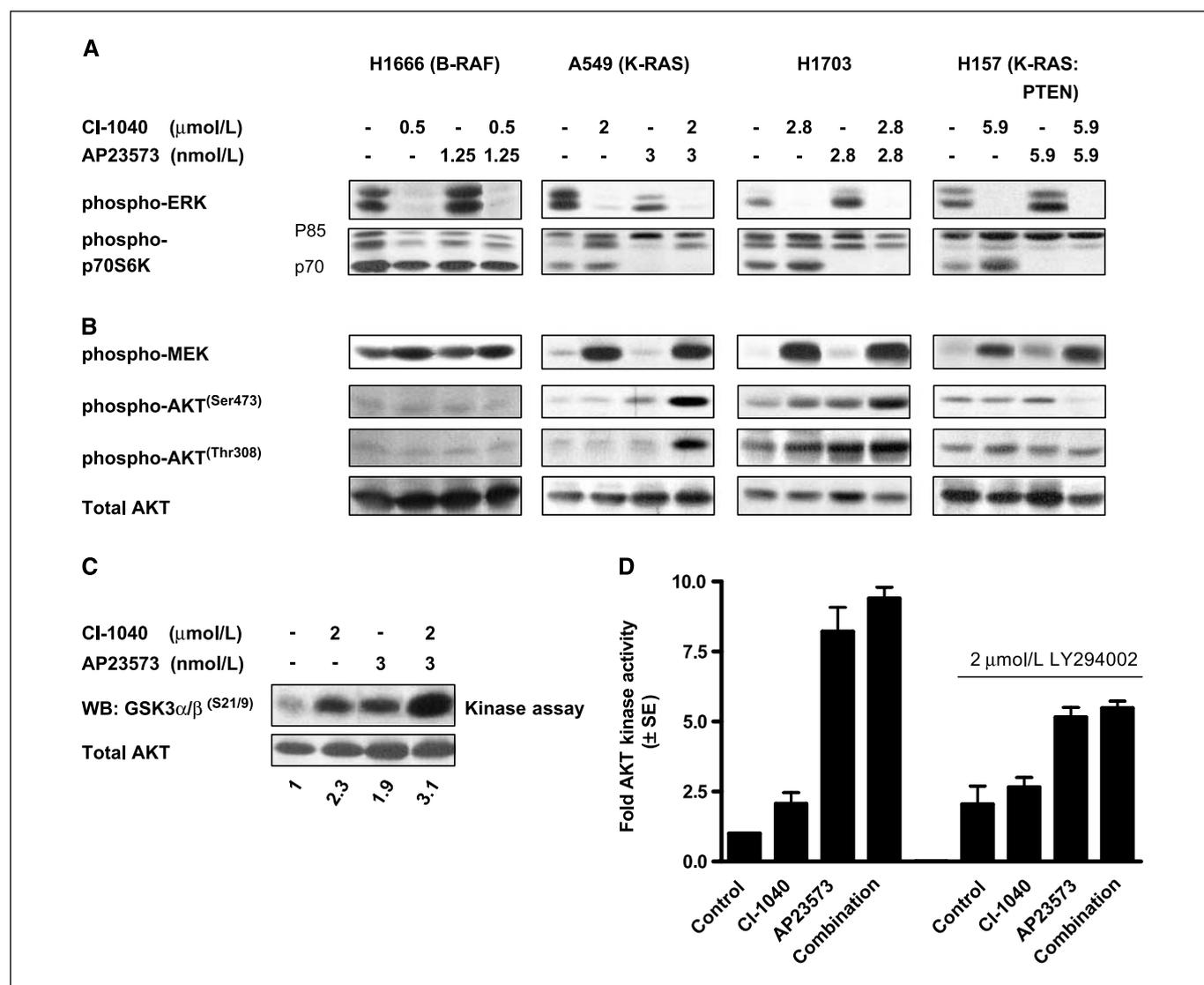
Figure 1. Effect of MEK and mTOR inhibitors on downstream components of RAS and AKT. Cells were treated with CI-1040 and AP23573, or concurrently with the combination of both, at doses that correspond to synergism. RAS, RAF, and PTEN genotypes are indicated. *A,* suppression of protein directly downstream of targets. *B,* expression of proteins involved in feedback regulation of RAS and mTOR signaling. *C,* CI-1040 and AP23573 induce AKT kinase in A549 NSCLC cells. Drug-treated A549 cells (24 h) were analyzed for AKT kinase activity by measuring the ability of AKT immunocomplexes to phosphorylate a GSK-3 fusion protein. Quantitation of AKT kinase activity, relative to pan-AKT, are shown. *D,* partial abrogation of CI-1040 and AP23573-induced AKT kinase by the PI3K inhibitor, LY294002. A549 cells were pretreated with either vehicle (*left*) or 2 μmol/L LY294002 (*right*) and subsequently treated with synergistic doses of CI-1040 (2 μmol/L) and AP23573 (3 nmol/L), alone or in combination for 24 h. Cells were processed for AKT kinase activity. *Columns,* values derived from duplicates and are means; *bars,* ± SE. AKT kinase activity was statistically significantly different in combination groups relative to CI-1040 but not AP23573.

Table 2. Cooperative suppression of cell proliferation by combined MEK and mTOR inhibition in NSCLC

Treatment	Doubling time (h)				
	Colo205 (B-RAF^{V600E})	H1666 (B-RAF^{G466V})	A549 (K-RAS^{G12S})	H1703*	H157* (K-RAS^{G12R} and PTEN^{G251C})
Control	27	62	21	57	34
CI-1040	173	120	32	84	125
AP23573	56	81	32	141	51
Combination	332	385	47	288	357

NOTE: Cells were seeded into 24-well plates and treated with CI-1040 and AP23573 alone, and in combination, at doses that resulted in synergism (see Fig. 2). After approximately three cell doublings, the number of adherent viable cells was determined using a coulter counter. The doubling time (h) was calculated according to the formula, t*ln(2)/ln(A/Ao), where A is the cell number at time t; Ao is the initial cell number. RAS, RAF, and PTEN genotypes are indicated.
*CA-AKT.

mechanism for the observed synergy *in vitro*. This finding is also substantiated by the doubling time experiments shown in Table 2 because cell number after three doublings was never less than the initial number of cells seeded, even in combination treatments.

Concurrent inhibition of MEK and mTOR suppresses protein translation. The 4E-BPs are downstream of mTORC1 and regulate cap-dependent translation by sequestering the translation initiation factor, eIF4E, via mTORC1-mediated phosphorylation. Three phosphorylated forms of 4E-BP1, γ, β, and α, in order of increasing electrophoretic mobility were resolved (Fig. 2*B*). A shift toward the α (hypophosphorylated) form of 4E-BP1 correlates with a reduced level of cap-dependent translation that permits 4E-BP1 to sequester eIF4E (33). The pattern of 4E-BP1 distribution differed among the four cell lines evaluated and cells with CA-AKT (H1703 and H157) had the highest expression. A shift in the phosphorylation state of the protein from γ to predominately αβ was observed in all cell lines treated with AP23573 (Fig. 2*B*), except H1666. This was confirmed by decreased phosphorylation of 4E-BP1$^{Ser65/Thr70}$; an effect that was potentiated by the CI-1040, especially in A549 and H157 cells, although concomitant decreases in steady-state levels of 4E-BP1 were also noted.

Ribosomal protein S6 is a substrate of p70S6K and forms part of the small ribosomal subunit that binds to the 18S rRNA very early in the assembly pathway leading to the 40S ribosome. In the 80S ribosome, it is localized at the interface between the subunits in a region where tRNA and protein factors catalyze mRNA translation (34). The function of ribosomal protein S6 is unclear, and it was once thought to regulate the translation of 5′-TOP mRNAs, although recently, this has been disproved (35). AP23573 alone dephosphorylated ribosomal protein S6$^{Ser235/236}$ in a dose-dependent manner in all cell lines (Fig. 2*A*). This was enhanced in the presence of CI-1040, such that phosphorylation of ribosomal protein S6$^{Ser235/236}$ was barely detectable in combination-treated cells, with minimal change in pan ribosomal protein S6 (Fig. 2*B*). Together with the effects on 4E-BP1, these data suggest integration of mTOR and RAS signaling on proteins that regulate protein translation.

MEK and mTOR inhibition cooperatively suppress polyribosomal synthesis and translation efficiency. To explore the effect of this drug combination on protein synthesis, drug-treated A549 cells were metabolically labeled with [^{35}S]methionine (Fig. 2*C*). AP23573 suppressed protein synthesis by 30% after

48 h of treatment, similar to what has been reported for rapamycin (36). CI-1040 also suppressed protein synthesis by ~15% after 48 h of treatment. The combination treatment resulted in a more marked suppression of protein synthesis by 50% after 48 h. This was also the case in H157 cells, although statistical significance was only achieved at 48 h, and unlike A549 cells, there was no effect of either CI-1040 or AP23573, either alone or in combination at 24 h.

Translationally inactive and/or underactive mRNAs are associated with a single ribosome, termed monosomes, whereas actively translated transcripts have two or more ribosomes associated with them and form oligosomes and polysomes. To investigate whether mRNA translation efficiency is suppressed by the inhibitors, total ribosomes were isolated from A549 cells. The total yield of ribosomes recovered for the various drug treatments at 3 and 24 h is summarized in Table 3. At 3 h, changes in total ribosomes were comparable for combination and AP23573-treated cells; however, by 24 h, there was a statistically significant difference in percentage of total ribosomes for combination treatments (~40%) compared with either CI-1040 or AP23573 alone. This is in agreement with [^{35}S]methionine incorporation data that also showed a decrease of 40% by 24 h in A549.

Monosomes and polysomes can be readily separated by sucrose gradient centrifugation, facilitating distinction between poorly and well-translated mRNAs. A representative experiment is shown in Fig. 2*D* that depicts the overall decrease in ribosome levels in combination-treated cells, as shown in Table 3. Changes in overall protein translation efficiency are reflected by changes in the polysome/monosome (P/M) ratio, whereby a redistribution of ribosomes to smaller oligomers and monosomes is observed. By 3 h, there was a trend for a reduced P/M ratio in combination-treated cells relative to either MEK or mTOR inhibition alone that became statistically significant by 24 h.

An alternative representation of the profile for A549 cells is provided that is normalized to equal amounts of ribosomes (Supplementary Fig. S3). Here, the relative distribution of polysome to monosomes is better represented, particularly, the increase in the monosome peak that is very apparent in combination-treated cells. This may be indicative of partial inhibition of translation initiation.

Rapamycin potentiated the antitumor efficacy of PD0325901 in animal models of human lung cancer. The effect of PD0325901, a highly specific MEK inhibitor, and the mTOR inhibitor, rapamycin, were evaluated in two human NSCLC tumor xenograft models, A549 and H157 (Fig. 3*A*), and heterotransplanted

human lung tumors grown in nude mice (Fig. 3*B*). Drugs were given for the duration of time represented on each graph. Mutations in B-RAF, KRAS, or NRAS were not detected in tumor DNA isolated from the tumors shown in three-dimensional; however, tumor cells were not microdissected, and conventional sequencing methodologies that are not highly sensitive were used.

PD0325901 and rapamycin have high selectivity for their respective targets, and importantly, both were available in the clinic at the time these studies were undertaken. The maximum-tolerated dose (MTD) in nude mice of PD0325901 (20 mg/kg qday p.o.) was also evaluated in heterotransplanted tumor models to compare the efficacy of the combination with high-dose PD0325901

monotherapy (Fig. 3*A*). Either drug alone caused varying degrees of growth suppression in the tumor models tested, except HTL-72, where daily low-dose PD0325901 prevented tumor growth for ~30 days. The combination enhanced antitumor efficacy relative to either dose of PD0325901 or rapamycin in all heterotransplanted lung tumor models tested, except H157. The effect of the combination was particularly impressive in HTL-72, where tumors were barely palpable after 60 days of treatment.

HTL-72 was derived from a former smoker. Tumors from these patients have a high frequency of K-RAS mutation (37). Although not detected by conventional sequencing, it is plausible that this tumor was mutant for either RAS or RAF because it had an

Figure 2. Combined MEK and mTOR inhibition suppresses proliferation, does not significantly potentiate cell death, and cooperatively suppresses 4EBP1 and S6 ribosomal–mediated protein translation. Cells were treated with CI-1040 and AP23573, or concurrently with the combination of both, at doses that correspond to synergism. *A,* the synergistic combination of MEK and mTOR inhibitors does not potentiate caspase-mediated cell death. *E*,* the predicted additive effect (percentage of caspase-mediated cell death) that was calculated using the data shown on the graph and applying the Loewe additivity effect model, whereby Effect E (drug A and B in combination) = (Effect A + Effect B) - (Effect A × Effect B). E is determined by expressing the proportion of caspase-positive cells as a scale of 1. The actual percentage of caspase-mediated cell death in combination treatments, as shown in the graph (*E observed*) was less than the predicted effect in all cell lines. *B,* expression of proteins implicated in the regulation of translation initiation. *C,* [^{35}S]methionine labeling of drug-treated cells. [^{35}S] incorporation into protein was determined for A549 cells and H157 drug-treated cells. Similar results were obtained for other NSCLC cell lines. *, statistical significance for the combination relative to CI-1040 and AP23573 alone. *NS,* not statistically significant. *D,* a representative profile of ribosomes isolated from equal amounts of S-30 proteins from drug-treated A549 cells is shown. Cells were exposed to drugs for 24 h. An alternative view, normalized for equal ribosomes, is shown in Supplementary Fig. S3.
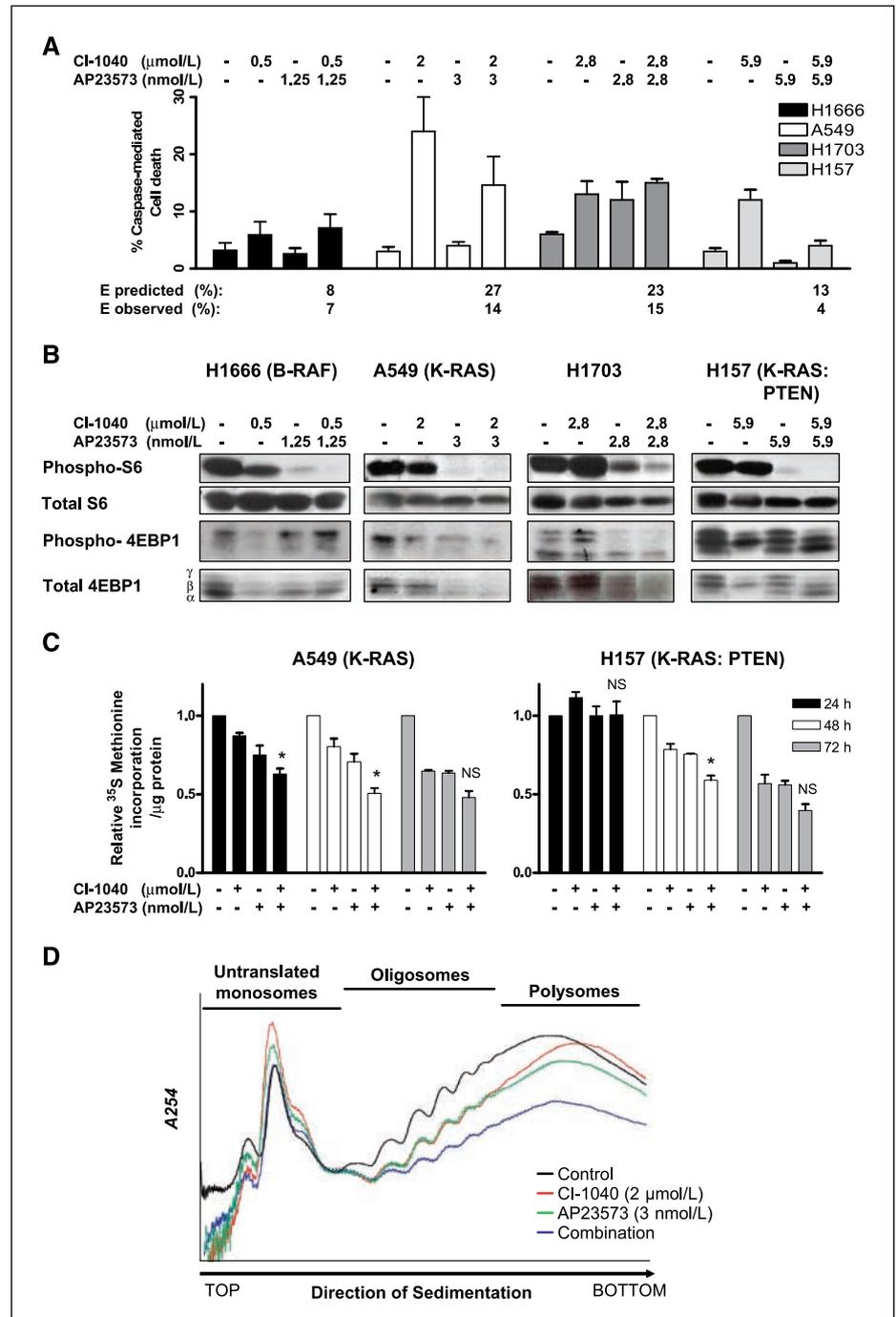
Table 3. Cooperative suppression of ribosomal biosynthesis and translation by combined MEK and mTOR inhibition

Treatment	Relative % ribosomes ($\pm$SE)		P/M ratio ($\pm$SE)	
	3 h ($n = 6$)	24 h ($n = 4$)	3 h ($n = 5$)	24 h ($n = 5$)
Control	100	100	3.86 ± 0.56	3.39 ± 0.36
CI-1040 (2 μmol/L)	99.2 ± 7.2	96.3 ± 7.8	3.52 ± 0.81	3.11 ± 0.39
AP23573 (3 nmol/L)	92.8 ± 10.6	84.7 ± 10.7	3.59 ± 0.70	3.04 ± 0.42
Combination	91.5 ± 8.9[NS]	58.9 ± 3.3*	3.40 ± 0.51[NS]	2.60 ± 0.38[†]

NOTE: Asynchronous A549 cells were treated with CI-1040 and AP23573 alone, and in combination, at doses that were synergistic. Total ribosomes were isolated and quantified, as described in Materials and Methods. Equal quantities of total ribosomes and/or S = 30 protein were resolved on 15% to 50% sucrose gradients to generate P/M profiles for each drug treatment (Fig. 2*D*). The P/M ratio, an index of translational efficiency, was determined as the ratio of the areas of translated polysomes to the areas of untranslated monosomes, using NIH image J. Statistical significance (two-tailed paired and unpaired Student's *t* tests to analyze P/M ratios and % ribosomes, respectively) is indicated for combination treatments relative to CI-1040 and AP23573 alone.
Abbreviation: NS, not significant.
*$P < 0.05$.
[†]$P < 0.01$.

excellent response to PD0325901 alone and sustained regressions in the combination-treated group. Those tumors treated with PD0325901 at the MTD grew more rapidly than the low-dose PD0325901 group; however, this effect was not observed in other models evaluated, although it is possible that this effect was specific to HTL-72. It may be due to nonspecific effects of PD0325901 at the MTD, resulting in feedback that counteracted antitumor effects at this dose.

Transient weight loss, hyperkeratosis, and mild diarrhea were noted at the commencement of dosing and after prolonged dosing
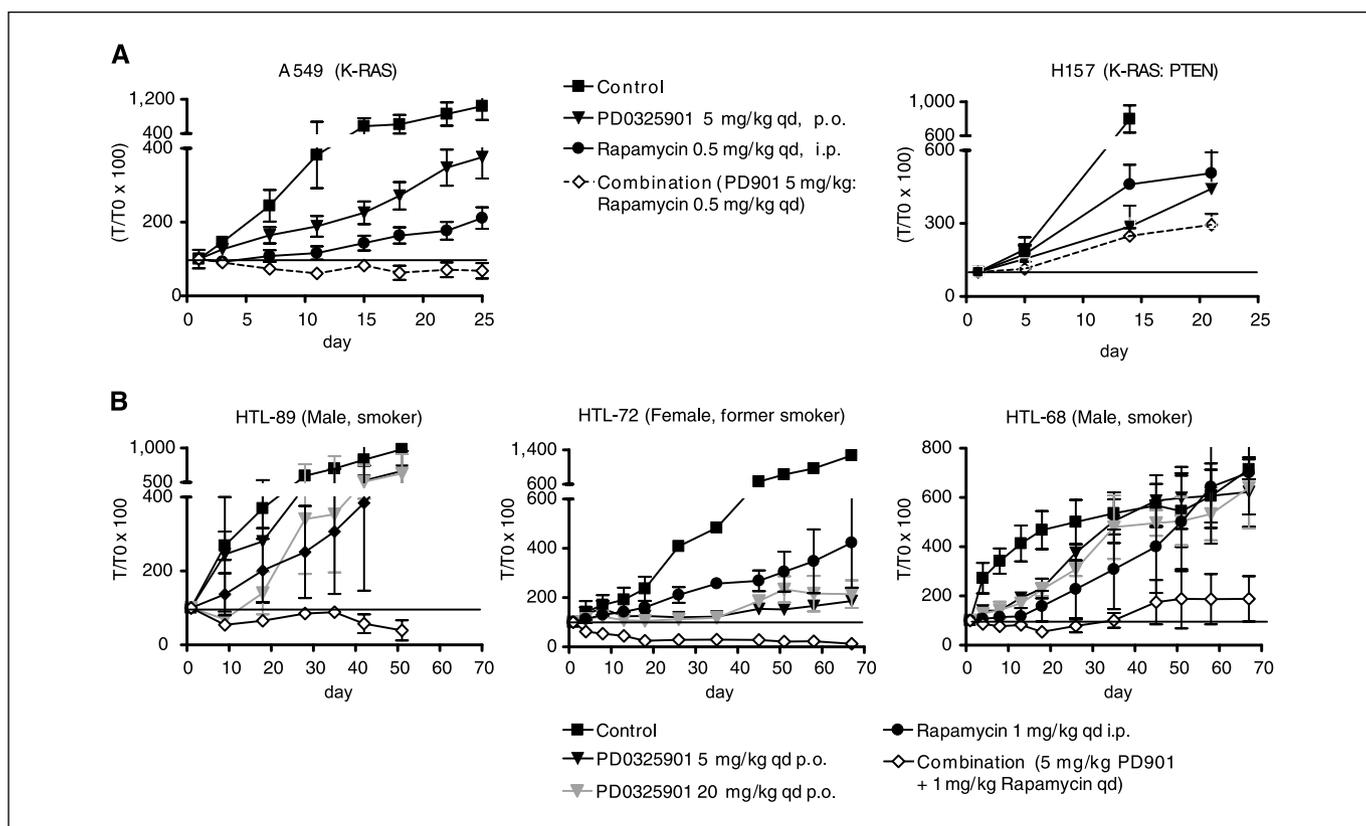
Figure 3. The combination of MEK and mTOR inhibition induces sustained regressions in NSCLC tumor models but not in the presence of constitutively active AKT. *A*, mice bearing A549 and H157 xenografts were randomized into groups and dosed with the drug schedules indicated. All drug combinations were administered concurrently, and no treatments were given on weekends. Dosing of animals with drugs continued until the termination of each experiment, as represented on the *x* axes. Data are expressed as percent change in initial tumor volume (T_0). *Horizontal black line,* initial tumor volume. *B,* As for *A,* except using human lung tumors heterotransplanted into nude mice. In addition to treatment with PD0325901 at 5 mg/kg, an additional cohort were given a higher dose of 20 mg/kg, MTD.

in combination and PD0325901 MTD groups (weight loss, ~7–12% for both). Mice were p.o. rehydrated until all mice in the group had complete resolution of symptoms. The longest lasting symptom was hyperkeratosis in combination-treatment groups, which necessitated p.o. rehydration for 3 to 10 days. Close follow-up of these symptoms in future experiments will be necessary to determine the underlying cause. Dose and schedule modifications may also be necessary to obviate the requirement for p.o. rehydration and further enhance the duration of tumor regression.

Discussion

Despite the genetic heterogeneity of lung cancer, we have shown that the combination of concurrent low-dose MEK and mTOR inhibitor therapy was synergistic, consistently suppressed cell proliferation in all lung cancer cell lines tested, and was associated with marked dephosphorylation of ribosomal protein S6$^{Ser235/236}$. These data substantiate the functional importance of integration points in signaling networks and, in the case of RAS and AKT-regulated translation, suggest that targeting of proteins at convergence points in signaling networks may be a useful strategy to circumvent both the emergence of drug resistance and upstream phamacogenomic variation. This does not preclude the possibility that tumors with distinct genotypes that are sensitive to MEK-inhibition alone (B-RAF or K-RAS mutant) will also have a more potent synergistic interaction with mTOR inhibitors.

Translation is the RNA-directed synthesis of polypeptides and is regulated at multiple checkpoints but primarily at initiation where eIFs recruit ribosomes to mRNA. The role of mTOR in translation regulation is well-documented (32, 38), but less is known about the effect of MAPK signaling on translation. The RAS pathway, via activated ERK, phosphorylates MAPK signal–integrating kinases (Mnk1 and 2; ref. 39) and p90 ribosomal S6 kinase (RSK; ref. 40) that directly and indirectly regulate eIF4E, respectively. Cooperation by this signaling network is further exemplified by the finding that RAS and AKT converge to phosphorylate eIF4B on Ser^{422}, via RSK activation and p70S6K (41). eIF4B is an RNA-binding protein that stimulates the ATPase and helicase activities of eIF4A (42). Furthermore, a recent study has reported RSK-mediated phosphorylation of ribosomal protein S6$^{Ser235/236}$ via a mTOR-independent mechanism, providing a more prominent role for RAS in the regulation of protein translation, via the preinitiation complex (43). These data are in excellent agreement with our results. The effects of MEK and mTOR inhibitors in the B-RAF mutant cells H1666 are intriguing and suggest a mTORC1-variant that is resistant to rapamycin-mediated dephosphorylation of 4E-BP1$^{Ser65/Thr70}$ and p70S6K^{Thr389} but responsive to alterations of ribosomal protein S6$^{Ser235/236}$ phosphorylation. It is plausible that RSK signaling is highly activated in these cells. Further evidence for this comes from the observation that MEK inhibition by CI-1040 caused dephosphorylation of 4E-BP1$^{Ser65/Thr70}$ and ribosomal protein S6$^{Ser235/236}$ in these cells.

Mechanistically, we propose a model by which inhibition of mTORC1, coupled to RSK suppression via MEK inhibition, synergistically suppresses ribosomal biosynthesis via a defect in translation initiation. The 43S preinitiation complex that is required for translation initiation contains ribosomal protein S6, 40S ribosomal subunit, GTP-eIF2-Met-tRNA, eIF3, eIF1, eIF1A, and eIF5 (44). Ribosomal protein S6$^{Ser235/236}$ phosphorylation was reproducibly suppressed by combined MEK and mTOR inhibition in all cell lines, pointing to a mechanism that perturbs formation of the preinitiation complex. The primary effect of the changes in translation initiation induced by the combination may be to alter translation efficiencies of many of the mRNAs that regulate both ribosomal biogenesis and cellular proliferation.

The growth inhibitory effects of concurrent mTOR and MEK suppression on proliferation that were consistently observed in cell lines with different RAS and AKT outputs (Table 2) underscores the biological importance of S6 ribosomal–mediated translation in regulating cell growth. These effects are similar to the phenotype observed in adult mice livers that have a conditionally deleted S6 gene, wherein cells failed to proliferate or induce cyclin E expression after partial hepatectomy (45). This suggests that the 40S ribosome, of which S6 is a component, functions as a highly conserved checkpoint that regulates cell cycle progression. A recent study of metastatic melanoma spheroids also showed growth arrest when PI3K and MEK inhibitors were used in combination and not alone (46). It is plausible that the combination of PI3K and/or AKT and MEK inhibitors will also be synergistic, although the mechanism of interaction described here may not apply to other combinations of MEK inhibitors, and the focus of this study was to use drugs that are already in the clinic. The *in vivo* toxicity of combinations of PI3K, or AKT inhibitors in combination with MEK inhibitors, is unknown at present. The low doses used in this study were well-tolerated in mice with manageable toxicities.

Importantly, the *in vitro* data summarized in Table 1 correctly predicted the sustained growth suppression observed in several lung tumor models, including primary lung tumors derived from patients, except in the PTEN-mutant xenograft model with CA-AKT (H157) that had delayed tumor growth but not regression. The discordance between *in vitro* and *in vivo* data for H157 is likely related to its highly vascularized phenotype and fast proliferation rate when grown in mice.

One of the major challenges of pharmacogenomic analyses that use cancer cell lines derived from patients is inherent genetic heterogeneity. Furthermore, the location and effect of different gene mutation may change, depending on the tissue type (7). >90% of B-RAF mutations reported in melanoma involve B-RAF^{V600E}, whereas most in NSCLC are non-V600. Herein, we confirmed the sensitivity of B-RAF^{V600E} cells to MEK-directed therapy, as previously described (6), and we also report that non-V600 B-RAF mutant lung cell lines have comparable sensitivity to MEK inhibitors as K-RAS mutants, although one cannot exclude the possibility that other lung-specific genetic or epigenetic alterations modulate the oncogenic activity of these mutants. Our data proposes a therapeutic role for MEK inhibitors in both B-RAF and K-RAS mutant lung tumors, except in the presence of CA-AKT, as shown by H1703 and H157.

In signaling networks, inhibition of one axis may be insufficient because other components compensate. There is concern that such effects may impede therapeutic efficacy, as shown for rapamycin-mediated AKT kinase activation (27). AKT signaling is highly pleiotropic, yet the drug-induced AKT kinase activation described herein was not associated with transcriptional activation of the forkhead transcription factors (data not shown). Despite the strong AKT kinase activation induced by the combination treatment in some cells, targets downstream of mTORC1 (4E-BP1, p70S6K, and S6 ribosomal protein) were suppressed, although it is plausible that the degree of synergy may be even more pronounced in the absence of AKT kinase activation. Interestingly, H1666 cells had no CI-1040– or AP2353-induced change in AKT phosphorylation or kinase activity (data not shown) and had an extremely strong synergistic interaction.

Two important paradigms are at the forefront of developing cancer therapeutics: first, the identification of signaling anomalies that confer dependence, and second, the appreciation that oncogenic signaling networks exhibit plasticity and redundancy. Therefore, rational drug targeting should be focused on proteins that integrate different components of a network. The mechanistic rationale for combining targeted therapies is complex, primarily because the functional relationship between disease, genetics, and targeted therapies is not well understood. This will require a greater understanding of the intricacies of feedback regulation and elucidation of as yet uncharacterized branches of the signaling network. By exploiting the intricate regulatory elements and integration points within such networks, we may be able to overcome the emergence of drug resistance that ensues when only one component of a network is suppressed and in addition to cancer, apply this concept to other diseases for which dysfunction of the RAS and PI3K/AKT signaling network is a hallmark.

References

1. Davies H, Hunter C, Smith R, et al. Somatic mutations of the protein kinase gene family in human lung cancer. Cancer Res 2005;65:7591–5.
2. Soria JC, Lee HY, Lee JI, et al. Lack of PTEN expression in non-small-cell lung cancer could be related to promoter methylation. Clin Cancer Res 2002;8:1178–84.
3. Marsit CJ, Zheng S, Aldape K, et al. PTEN expression in non-small-cell lung cancer: evaluating its relation to tumor characteristics, allelic loss, and epigenetic alteration. Hum Pathol 2005;36:768–76.
4. Samuels Y, Wang Z, Bardelli A, et al. High frequency of mutations of the PIK3CA gene in human cancers. Science 2004;304:554.
5. Weinstein IB. Cancer. Addiction to oncogenes-the Achilles heal of cancer. Science 2002;297:63–4.
6. Solit DB, Garraway LA, Pratilas CA, et al. BRAF mutation predicts sensitivity to MEK inhibition. Nature 2006;439:358–62.
7. Davies H, Bignell GR, Cox C, et al. Mutations of the BRAF gene in human cancer. Nature 2002;417:949–54.
8. Wan PT, Garnett MJ, Roe SM, et al. Mechanism of activation of the RAF-ERK signaling pathway by oncogenic mutations of B-RAF. Cell 2004;116:855–67.
9. Brose MS, Volpe P, Feldman M, et al. BRAF and RAS mutations in human lung cancer and melanoma. Cancer Res 2002;62:6997–7000.
10. Rinehart J, Adjei AA, Lorusso PM, et al. Multicenter phase II study of the oral MEK inhibitor, CI-1040, in patients with advanced non-small-cell lung, breast, colon, and pancreatic cancer. J Clin Oncol 2004;22:4456–62.
11. Lorusso PM, Adjei AA, Varterasian M, et al. Phase I and pharmacodynamic study of the oral MEK inhibitor CI-1040 in patients with advanced malignancies. J Clin Oncol 2005;23:5281–93.
12. Sebolt-Leopold JS, Herrera R. Targeting the mitogen-activated protein kinase cascade to treat cancer. Nat Rev Cancer 2004;4:937–47.
13. Vivanco I, Sawyers CL. The phosphatidylinositol 3-kinase AKT pathway in human cancer. Nat Rev Cancer 2002;2:489–501.
14. Thimmaiah KN, Easton JB, Germain GS, et al. Identification of N10-substituted phenoxazines as potent and specific inhibitors of Akt signaling. J Biol Chem 2005;280:31924–35.
15. Burns S, Travers J, Collins I, et al. Identification of small-molecule inhibitors of protein kinase B (PKB/AKT) in an αScreenTM high-throughput screen. J Biomol Screen 2006.
16. Guertin DA, Sabatini DM. Defining the role of mTOR in cancer. Cancer Cell 2007;12:9–22.
17. Sawyers CL. Will mTOR inhibitors make it as cancer drugs? Cancer Cell 2003;4:343–8.
18. Easton JB, Houghton PJ. Therapeutic potential of target of rapamycin inhibitors. Expert Opin Ther Targets 2004;8:551–64.
19. Dilling MB, Germain GS, Dudkin L, et al. 4E-binding proteins, the suppressors of eukaryotic initiation factor 4E, are down-regulated in cells with acquired or intrinsic resistance to rapamycin. J Biol Chem 2002;277:13907–17.
20. Desai AA, Janisch L, Berk LR, et al. A phase I trial of a novel mTOR inhibitor AP23573 administered weekly (wkly) in patients (pts) with refractory or advanced malignancies: a pharmacokinetic (PK) and pharmacodynamic (PD) analysis [2004 ASCO Annual Meeting Proceedings (Post-Meeting Edition)]. J Clin Oncol 2004;22:3150.
21. Dougherty MK, Muller J, Ritt DA, et al. Regulation of Raf-1 by direct feedback phosphorylation. Mol Cell 2005;17:215–24.
22. Zimmermann S, Moelling K. Phosphorylation and regulation of Raf by Akt (protein kinase B). Science 1999;286:1741–4.
23. Roux PP, Ballif BA, Anjum R, Gygi SP, Blenis J. Tumor-promoting phorbol esters and activated Ras inactivate the tuberous sclerosis tumor suppressor complex via p90 ribosomal S6 kinase. Proc Natl Acad Sci U S A 2004;101:13489–94.
24. Ma L, Chen Z, Erdjument-Bromage H, Tempst P, Pandolfi PP. Phosphorylation and functional inactivation of TSC2 by Erk implications for tuberous sclerosis and cancer pathogenesis. Cell 2005;121:179–93.
25. Skehan P, Storeng R, Scudiero D, et al. New colorimetric cytotoxicity assay for anticancer-drug screening. J Natl Cancer Inst 1990;82:1107–12.
26. Chou TC, Talalay P. Quantitative analysis of dose-effect relationships: the combined effects of multiple drugs or enzyme inhibitors. Adv Enzyme Regul 1984;22:27–55.
27. O'Reilly KE, Rojo F, She QB, et al. mTOR inhibition induces upstream receptor tyrosine kinase signaling and activates Akt. Cancer Res 2006;66:1500–8.
28. Koritzinsky M, Magagnin MG, van den Beucken T, et al. Gene expression during acute and prolonged hypoxia is regulated by distinct mechanisms of translational control. EMBO J 2006;25:1114–25.
29. McDaid HM, Lopez-Barcons L, Grossman A, et al. Enhancement of the therapeutic efficacy of taxol by the mitogen-activated protein kinase kinase inhibitor CI-1040 in nude mice bearing human heterotransplants. Cancer Res 2005;65:2854–60.
30. Brognard J, Clark AS, Ni Y, Dennis PA. Akt/protein kinase B is constitutively active in non-small-cell lung cancer cells and promotes cellular survival and resistance to chemotherapy and radiation. Cancer Res 2001;61:3986–97.
31. Forgacs E, Biesterveld EJ, Sekido Y, et al. Mutation analysis of the PTEN/MMAC1 gene in lung cancer. Oncogene 1998;17:1557–65.
32. Bjornsti MA, Houghton PJ. The TOR pathway: a target for cancer therapy. Nat Rev Cancer 2004;4:335–48.
33. von Manteuffel SR, Gingras AC, Ming XF, Sonenberg N, Thomas G. 4E-BP1 phosphorylation is mediated by the FRAP-p70s6k pathway and is independent of mitogen-activated protein kinase. Proc Natl Acad Sci U S A 1996;93:4076–80.
34. Nygard O, Nika H. Identification by RNA-protein cross-linking of ribosomal proteins located at the interface between the small and the large subunits of mammalian ribosomes. EMBO J 1982;1:357–62.
35. Pende M, Um SH, Mieulet V, et al. S6K1(−/−)/S6K2(−/−) mice exhibit perinatal lethality and rapamycin-sensitive 5′-terminal oligopyrimidine mRNA translation and reveal a mitogen-activated protein kinase-dependent S6 kinase pathway. Mol Cell Biol 2004;24:3112–24.
36. Grolleau A, Bowman J, Pradet-Balade B, et al. Global and specific translational control by rapamycin in T cells uncovered by microarrays and proteomics. J Biol Chem 2002;277:22175–84.
37. Shigematsu H, Takahashi T, Nomura M, et al. Somatic mutations of the HER2 kinase domain in lung adenocarcinomas. Cancer Res 2005;65:1642–6.
38. Gera JF, Mellinghoff IK, Shi Y, et al. AKT activity determines sensitivity to mammalian target of rapamycin (mTOR) inhibitors by regulating cyclin D1 and c-myc expression. J Biol Chem 2004;279:2737–46.
39. Parra JL, Buxade M, Proud CG. Features of the catalytic domains and C termini of the MAPK signal-integrating kinases Mnk1 and Mnk2 determine their differing activities and regulatory properties. J Biol Chem 2005;280:37623–33.
40. Roux PP, Richards SA, Blenis J. Phosphorylation of p90 ribosomal S6 kinase (RSK) regulates extracellular signal-regulated kinase docking and RSK activity. Mol Cell Biol 2003;23:4796–804.
41. Shahbazian D, Roux PP, Mieulet V, et al. The mTOR/PI3K and MAPK pathways converge on eIF4B to control its phosphorylation and activity. Embo J 2006;25:2781–91.
42. Gingras AC, Raught B, Sonenberg N. eIF4 initiation factors: effectors of mRNA recruitment to ribosomes and regulators of translation. Annu Rev Biochem 1999;68:913–63.
43. Roux PP, Shahbazian D, Vu H, et al. RAS/ERK signaling promotes site-specific ribosomal protein S6 phosphorylation via RSK and stimulates cap-dependent translation. J Biol Chem 2007;282:14056–64.
44. Westermann P, Nygard O. Cross-linking of mRNA to initiation factor eIF-3, 24 kDa cap binding protein and ribosomal proteins S1, S3/3a, S6 and S11 within the 48S pre-initiation complex. Nucleic Acids Res 1984;12:8887–97.
45. Volarevic S, Stewart MJ, Ledermann B, et al. Proliferation, but not growth, blocked by conditional deletion of 40S ribosomal protein S6. Science 2000;288:2045–7.
46. Smalley KS, Haass NK, Brafford PA, Lioni M, Flaherty KT, Herlyn M. Multiple signaling pathways must be targeted to overcome drug resistance in cell lines derived from melanoma metastases. Mol Cancer Ther 2006;5:1136–44.

AACR American Association for Cancer Research

Targeting Protein Translation in Human Non−Small Cell Lung Cancer via Combined MEK and Mammalian Target of Rapamycin Suppression

Marie-Emmanuelle Legrier, Chia-Ping Huang Yang, Han-Guang Yan, et al.

Updated version	Access the most recent version of this article at: http://cancerres.aacrjournals.org/content/67/23/11300
Supplementary Material	Access the most recent supplemental material at: http://cancerres.aacrjournals.org/content/suppl/2007/11/21/67.23.11300.DC1

Cited articles	This article cites 45 articles, 24 of which you can access for free at: http://cancerres.aacrjournals.org/content/67/23/11300.full#ref-list-1
Citing articles	This article has been cited by 16 HighWire-hosted articles. Access the articles at: http://cancerres.aacrjournals.org/content/67/23/11300.full#related-urls

E-mail alerts	Sign up to receive free email-alerts related to this article or journal.
Reprints and Subscriptions	To order reprints of this article or to subscribe to the journal, contact the AACR Publications Department at pubs@aacr.org.
Permissions	To request permission to re-use all or part of this article, use this link http://cancerres.aacrjournals.org/content/67/23/11300. Click on "Request Permissions" which will take you to the Copyright Clearance Center's (CCC) Rightslink site.